Transportable automated ammonia sensor based on a pulsed thermoelectrically cooled quantum-cascade distributed feedback laser

Anatoliy A. Kosterev, Robert F. Curl, Frank K. Tittel, Rüdeger Köhler, Claire Gmachl, Federico Capasso, Deborah L. Sivco, and Alfred Y. Cho

A compact ammonia sensor based on a 10-μm single-frequency, thermoelectrically cooled, pulsed quantum-cascade laser with an embedded distributed feedback structure has been developed. To measure NH_3 concentrations, we scanned the laser over two absorption lines of its fundamental ν_2 band. A sensitivity of better than 0.3 parts per million was achieved with just a 1-m optical path length. The sensor is computer controlled and automated to monitor NH_3 concentrations continuously for extended periods of time and to store data in the computer memory. © 2002 Optical Society of America

OCIS codes: 140.5960, 280.3420, 300.6320.

1. Introduction

Sensitive, compact devices for the quantification of trace gases are required for a number of applications that include industrial process control, environmental monitoring, and noninvasive medical diagnostics. A well-established technique for detecting molecular species in the gas phase is high-resolution infrared absorption spectroscopy. Until recently, real-world applications of this method were limited because of the absence of convenient tunable coherent light sources in the mid-IR region (3–20 μm), where the fundamental absorption bands of most molecules are located. This situation has changed with the development of quantum-cascade (QC) lasers,[1,2] especially single-frequency devices with an embedded distributed feedback (DFB) structure. QC DFB lasers are capable of delivering tens and for certain devices even hundreds of milliwatts of narrow-linewidth mid-IR radiation. QC lasers can be operated in a pulsed mode up to and above room temperature, which is of particular interest for real-world gas-sensing appli-

cations, because it eliminates the bulkiness and cost of an optical cryostat and cryogenic consumables (liquid nitrogen). The first laboratory demonstration of sensitive absorption spectroscopy with a pulsed QC DFB laser was reported in Ref. 3, where wavelength modulation was used to improve the signal-to-noise ratio. Application of the direct absorption technique with a pulsed QC DFB laser for trace gas detection in ambient air was first described in Ref. 4. Here we report details of the design and performance of a robust, portable ammonia sensor based on a pulsed QC DFB laser that operates at ~10 μm. This sensor has been successfully applied to dynamic ammonia concentration monitoring of bioreactor vent gases at the NASA Johnson Space Center, Houston, Texas.

2. Gas Sensor Description

To detect NH_3, we selected the absorption lines ${}^aR_1(2)$ at 992.4503 cm^{-1} and ${}^aR_0(2)$ at 992.6988 cm^{-1} (~10.1 μm) in the ν_2 fundamental absorption band. These lines are strong, well resolved at pressures below 200 Torr, and are free from interference by water and other air components absorption. The pulsed QC DFB laser available for this study accessed this wavenumber region when operated at a temperature of −11.7 °C.

Ultrasensitive ammonia detection in this spectral region with a pulsed QC DFB laser was reported previously in Ref. 5. McManus *et al.*[5] used a multipass cell with a 209-m effective path length and two IR detectors to achieve improved detection sensitivity. Our emphasis in this study is to achieve mod-

A. A. Kosterev (akoster@rice.edu), R. F. Curl, and F. K. Tittel are with the Rice Quantum Institute, Rice University, Houston, Texas 77251-1892. R. Kohler, C. Gmachl, F. Capasso, D. L. Sivco, and A. Y. Cho are with Bell Laboratories, Lucent Technologies, 600 Mountain Avenue, Murray Hill, New Jersey 07974.
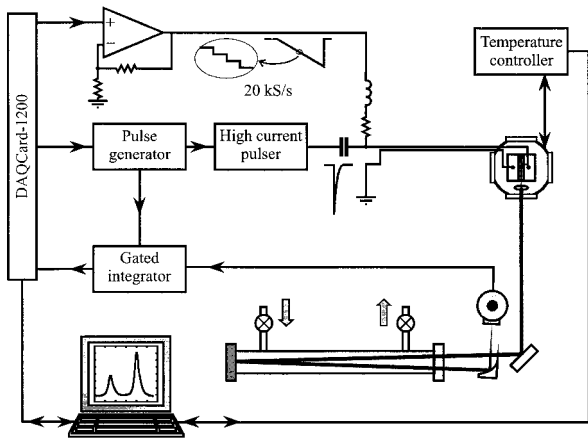
Fig. 1. Schematic of a QC DFB laser-based ammonia sensor; the subthreshold current is updated at a rate of 20 kilosamples per second (kS/s), synchronously with the laser pulses.

erate [sub-ppm (parts per million)] sensitivity levels with a simple and cost-effective sensor platform (i.e., a single detector and no multipass gas cell).

The NH_3 sensor design is shown schematically in Fig. 1. The QC DFB laser was mounted on top of a three-stage thermoelectric unit (Melcor 3CP), inside a vacuum-tight housing with overall dimensions of $100 \text{ mm} \times 160 \text{ mm} \times 180 \text{ mm}$ (depicted in Fig. 2), and assembled from commercially available vacuum and optomechanical components. To remove the heat generated by operation of the Peltier cooler, the bottom of the thermoelectric unit was soldered to a water-cooled housing base. A temperature controller (Wavelength Electronics LFI-3751 TE) was used to set and monitor the laser temperature. With this
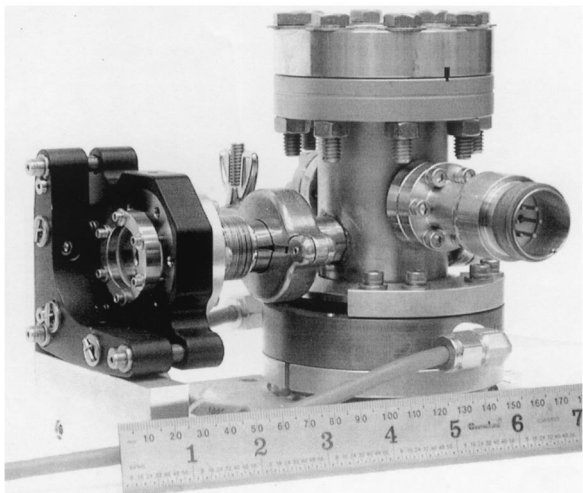
Fig. 2. Photograph of the vacuum-tight pulsed QC DFB laser housing. The laser is mounted inside on a three-stage thermoelectric element. Observation windows on top and opposite the beam output facilitate alignment of the collimating lens ($f = 3$ mm, 6 mm diameter). The bottom of the housing is made of copper for better thermal conductivity. It is soldered to the thermoelectric element and can be water cooled.

arrangement, the operating QC DFB laser could be cooled to $-55 \,°C$.

We collimated the laser emission by using an aspheric antireflection-coated ZnSe lens with a focal length of 3 mm and a diameter of 6 mm mounted inside the housing. The lens position could be adjusted externally. The collimated laser light emerged from the housing through a 30-arc min wedged antireflection-coated ZnSe window and was directed into a 0.5-m-long optical gas cell. This cell consisted of a glass tube fitted with Teflon valves and stainless steel window holders based on commercial NW16CF vacuum flanges. One end of the cell was equipped with a 30-arc min wedged antireflection-coated ZnSe window and the other with a SiO protected flat Al mirror (both 25.4 mm diameter). This resulted in a two-pass configuration with a total optical path length of 1 m. The exiting beam was focused onto a liquid-nitrogen-cooled HgCdTe detector with a built-in preamplifier (Kolmar KMPV10-1-J1/DC, 20-MHz bandwidth) by means of a 25.4-mm-diameter off-axis parabolic mirror. The utilization of a cryogenic detector does not imply strong limitations to the sensor performance, because it uses only a small amount of liquid nitrogen and has a holding time of ~15 h. In the future, we envision the use of a thermoelectrically cooled detector. The air to be analyzed flowed continuously through the absorption cell at a low controlled flow rate. The relatively slow flow was necessary because the bioreactor vent system permitted gas sampling only at a 10 SCCM or lower rate. (SCCM denotes cubic centimeters per minute at STP.) A pressure controller was used to maintain the pressure inside the cell at 95 Torr. The laser housing, optical gas cell, gas flowmeter, pressure controller, IR detector, visible diode laser for alignment, and optical components were mounted on a $30.5 \text{ cm} \times 61 \text{ cm}$ aluminum breadboard.

3. Data Acquisition and Analysis

The laser current was supplied in 5-ns-long, ~4-A peak current pulses at a 20-kHz repetition rate as described in Ref. 4. A compact driver (Directed Energy PCO-7110 Model 40-4) was used for the QC DFB laser excitation, and a computer-controlled subthreshold current pedestal was added to each pulse to set the optical pulse frequency. By appropriate ramping of the subthreshold current, 512 laser pulses at a 20-kHz repetition rate scanned the desired spectral range. The tuning voltage that defines the subthreshold current was applied in the shape of a linear ramp with an offset to compensate for the initial bias of the QC laser. A DAQ-1200 data-acquisition card and LabView software (National Instruments) were used to trigger the laser pulser, to set the subthreshold current, and to acquire the spectral data. The number of pulses in a scan was limited by the capabilities of this card. The repetition rate was limited by the gated integrator (Stanford Research Systems Model SR250) used as an interface between the fast IR detector
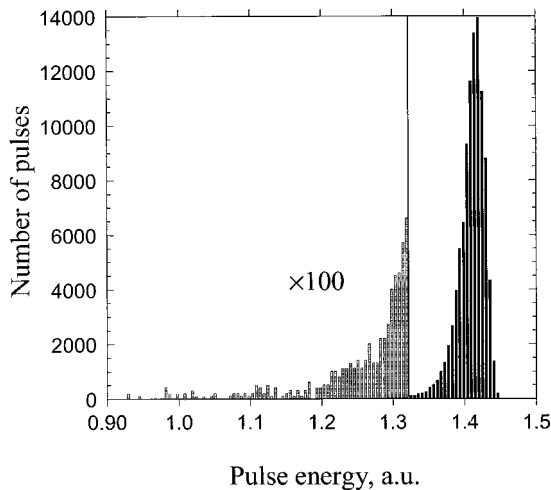
Fig. 3. Energy distribution in a sample of 100,000 laser pulses with the laser excitation current fixed.

and the data-acquisition card. The scans followed each other with ~50% duty cycle because of computer software and hardware limitations. In most sensor runs the data were analyzed to determine the NH_3 concentration after we acquired and averaged 400 scans, and the measurement sequence was repeated every 4 min.

It was found that, at a fixed amplitude of the excitation current pulse, the output energy distribution of this particular QC DFB laser exhibited an asymmetrical shape with a long low-energy tail (Fig. 3). This tail increased the statistical error of the averaged signal. The distribution was narrower at a higher laser current, but at the same time the laser linewidth became broader and less symmetric. A special software procedure was implemented to suppress the influence of the low-energy laser pulses. The intensity of each pulse $I(i,n)$ in the n-th scan was digitized and stored in the computer memory; here i is the pulse number in a scan. This was repeated until a specified number of scans was acquired. Then for each i the maximum $I_{max}(i)$ was found, and all the pulses with $I(i, n) < 0.93I_{max}(i)$ were disregarded. At typical settings of the laser current the percentage of discarded pulses was ~5%. Figure 3 corresponds to a slightly higher laser current and therefore narrower distribution. Finally, the remaining pulses were averaged for each i to obtain $I_{av}(i)$. This selection procedure was found to reduce the noise in the averaged spectra by a factor of 4, when 1000 scans were collected.

The position of NH_3 absorption lines provided an absolute frequency reference for frequency calibration. The frequency scale was linearized by means of interference fringes from two air-separated uncoated ZnSe surfaces. The scan length was set to 0.75 cm^{-1} to observe the 992.4503- and 992.6988- cm^{-1} lines simultaneously. By using data acquired at relatively high NH_3 concentration, we determined that the QC laser possessed a linewidth of ~0.02

cm^{-1} with an asymmetric shape. This broad, asymmetric laser line shape makes traditional analysis of spectra by fitting the lines with either Lorentz or Voigt functions inapplicable. Instead, we used the following procedure:

(1) A reference spectrum in terms of base e absorbance was acquired with a N_2:NH_3 mixture that contained ~100 parts per million (ppm) of NH_3. We determined the actual concentration of NH_3 in this reference sample by comparing the area of the absorption lines [$\int \alpha dv$, where α (cm^{-1}) is the absorption coefficient] to the area predicted by the HITRAN database for the same temperature. The spectrum was then stored in the computer memory as a function $y_i = f(i)$, where i is a data point number (that is, the number of the corresponding laser pulse in the frequency scan). This function results from convolution of the real absorption spectrum and the laser line shape.

(2) We acquired spectral data $I_{av}(i)$ as described above with the gas sample containing an unknown concentration of NH_3 at the same pressure and temperature.

(3) Using a high concentration reference spectrum, we defined three (almost) absorption-free parts of the spectral scan (i.e., between and at each side of the two NH_3 absorption lines). We determined the baseline of the spectral data of the unknown gas sample by fitting a sixth-order polynomial to the corresponding segments of $I_{av}(i)$. Fractional absorption y_i of the unknown sample was computed through subtraction of $i_{(av)}(i)$ from the baseline with subsequent normalization to the baseline. Because the absorbance was small for the unknown spectrum, conversion to base e absorbance was not needed.

(4) The best fit of the sample fractional absorption by the function

$$y_i (Bf(i - x) + b \tag{1}$$

was found. Parameter x was introduced to compensate for slow drift of the line positions on the scan because of slight variations of the laser temperature, and the b parameter partially helps to correct for an error in the baseline interpolation. Usually the fit resulted in $b \approx 0$. Parameter B yields the concentration in the test gas sample relative to the reference gas sample.

To perform the fit in step (4) we modified a LabView procedure, *Nonlinear Lev-Mar Fit.vi*, so that it could use a tabulated function instead of an analytic expression. An example of the fitted data is presented in Fig. 4. This spectrum corresponds to 6.7 ppm of NH_3 and was acquired with 400 frequency scans. The standard single-point deviation of the fit is $\sigma = 7.14 \times 10^{-4}$ fractional absorbance (with a 10-s data-acquisition time).

In Ref. 3 Namjou *et al*. stated that the single-point sensitivity was 5×10^{-5} Hz$^{-1/2}$ at a 1-MHz laser pulse repetition rate. Fluctuations of the laser pulse energy are the primary sources of noise in
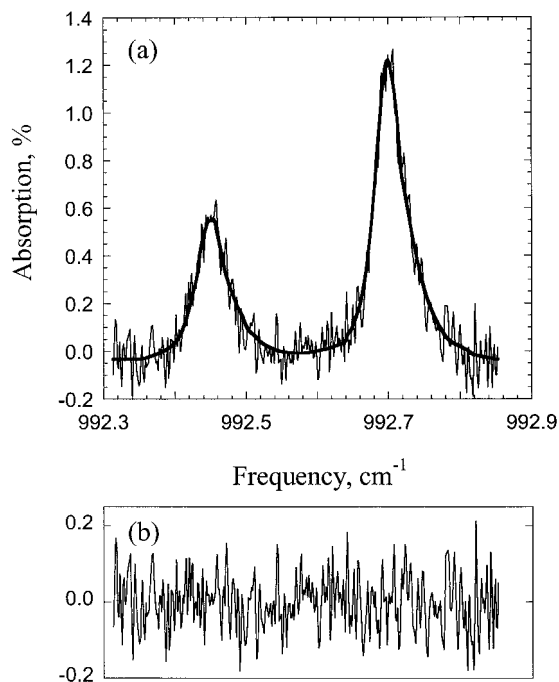
Fig. 4. (a) Example of an acquired data set after automated baseline correction and fitting with the previously tabulated function; see Section 3. The fitting yielded a 6.7-ppm NH_3 concentration in the sample. The fit residual is shown in (b).

Fig. 5. Time dependence of the NH_3 concentration in a gas flow measured simultaneously by two spectroscopic gas sensors: the mid-IR QC DFB sensor ($\bigcirc$) and a diode-laser overtone sensor (x). The flow was produced in a gas-mixing system that combined pure nitrogen with 100-ppm NH_3-doped nitrogen. The mid-IR QC DFB laser-based sensor exhibits higher inertia because of the longer tubing that connects it to the gas source.

our measurements. Thus the error decreases as a square root of the number of averaged laser pulses, and a proper comparison of our results with the sensitivity reported in Ref. 3 requires a normalization to the repetition frequency (i.e., the square root of the frequency ratio). This results in a 1-MHz equivalent sensitivity of $\sigma' = 3.2 \times 10^{-4}$ $Hz^{-1/2}$. Almost 1 order of magnitude better sensitivity as described in Ref. 3 is due to suppression of laser noise by use of a wavelength modulation technique (also different specimens of QC DFB lasers exhibit different energy fluctuations). This approach, however, is experimentally more complex and does not permit direct concentration measurements. Alternatively two-channel detection can be used if improved sensitivity is required for a specific application. In a separate experiment we could obtain at least one order of sensitivity gain by normalization to a reference channel.

A value that is more important in gas detection applications is the accuracy in the measurement of the absorption line area, because this area is directly related to the species concentration and does not depend on the laser linewidth. This accuracy can be readily derived with some simplifying assumptions. Parameter x in the fitting equation (1) makes the fit nonlinear. However, it changed slowly and was preset to its quasi-constant value at the beginning of a measurement run. To simplify the estimation of the error in the concentration resulting from the procedure described above, we assume that it is fixed and

that $b \equiv 0$. Then the fitting becomes a linear regression and Eq. (A7) in Ref. 6 applies. It yields

$$\delta A = \sigma \left[\frac{\Delta \nu}{\int g^2(\nu)d\nu} \right]^{1/2}, \qquad (2)$$

where δA is the standard error of $A = \int \alpha l d\nu$, l is the path length; $\Delta \nu$ is the frequency scan resolution, and $g(\nu)$ is the absorption spectrum normalized by the condition $\int g(\nu)d\nu = 1$. The function $g(\nu)$ describes the shape of the reference spectrum $f(i)$. For our data, $\Delta \nu = 1.5 \times 10^{-4}$ cm^{-1} and a numerical integration gives $\int g^2(\nu)d\nu = 5.27$ cm. Equation (2), yields $\delta A = 1.2 \times 10^{-4}$ cm^{-1}, which converts to a standard error in concentration $\delta[NH_3] = 70$ parts per billion.

We also performed an intercomparison study of two distinct ammonia sensors: the one we describe in this paper and an overtone-based near-IR detector that operates at 1.53 μm with a 36-m multipass cell as reported in Refs. 7 and 8. We calculated NH_3 concentrations from the absorption spectra using the HITRAN spectroscopic database[9] for the QC-based sensor and by using the data in Ref. 10 for the near-IR gas sensor. The results are shown in Fig. 5. Both sensors were connected to the same source, which was a gas dilution system that mixes pure nitrogen with a 100-ppm NH_3-doped nitrogen. The flow rate for both sensors was set to ~10 SCCM to simulate sampling from the bioreactor vent system. The length of tubing from the gas source to the QC-based gas sensor was ~4 m longer than that to the near-IR sensor because of space requirements. This added some inertia to the QC detector response as is evident from the plot presented in Fig. 5. However, the steady-state concentration data from both sen-

sors are almost identical. The accuracy of the near-IR sensor is somewhat better because of its 36 times longer path length and much lower laser noise for the cw 1.53-μm telecommunications DFB laser diode, which was further suppressed by balanced radiometric detection. The observed scatter of the measured [NH$_3$] was ~0.6 ppm peak to peak, which corresponds to a δ[NH$_3$] ≈ 150 parts per billion. The additional error, compared with the estimated one obtained from Eq. (2) is due mainly to the uncertainty of the baseline, which Eq. (2) does not take into account. In addition some fitting procedure parameters had not been optimized at the time of this experiment.

Real-time determination of the actual trace gas concentration in a system such as the atmosphere or bioreactor we report in this paper can be made more accurate if we take into account intrinsic system properties. In our case, the short time fluctuations in the measured concentration reflect the sensor properties and not the behavior of the gas concentration in the system. For this system, the actual NH$_3$ concentration is not expected to exhibit stochastic fluctuations every 4 min as measurements are performed. Changes in the bioreactor occur on a time scale of hours. Ammonia absorption and desorption from the walls of the tubing that connect the sensor to the system add further inertia to the measurements. Therefore, mathematical filtering that removes part of the high-frequency variations from one measurement to the next should improve the measurement accuracy. To discern slow trends in concentration in real time, a Kalman filtering technique[11] can be applied to trace gas measurements for various slow-changing systems. With an appropriate choice of filter parameters, such filtering has been shown to reduce the scatter significantly.[12,13] An important advantage of the Kalman filter over more common averaging techniques is that it keeps track of the whole measurement history without keeping all the previous data in memory and acts in real time, thereby providing a corrected concentration value after each measurement. It is especially useful if the measured concentration is used to control the system through a feedback loop.

A set of measurements that illustrate the application of Kalman filtering by use of a QC sensor is shown in Fig. 6. Initially ambient air was sampled, and the measured concentration was zero because air contains negligible amounts of ammonia. A cylinder containing 100 ppm of NH$_3$ in N$_2$ was then connected to the sensor for several minutes. A subsequent cleaning of the sensor by flowing ambient air at a low (10-SCCM) rate provided a concentration decay that was monitored for ~15 h. From the data presented in Fig. 6, we conclude that the detector sensitivity is better than 0.3 ppm without Kalman filtering. The simplest Kalman filter procedure[13] applied to these data reduced the NH$_3$ concentration uncertainty to ±0.04 ppm.

The QC DFB laser-based NH$_3$ sensor described here was used to monitor NH$_3$ concentration levels
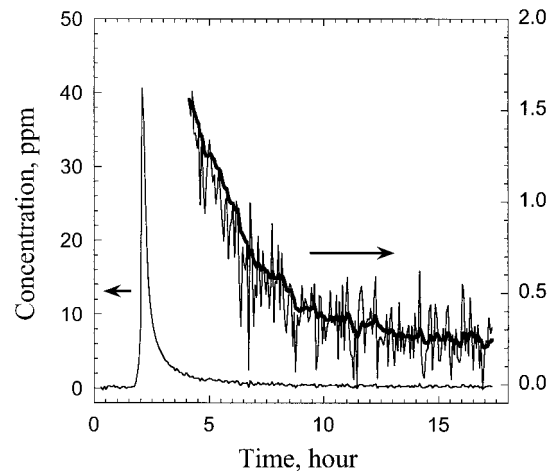
Fig. 6. Relaxation behavior of NH$_3$ concentration as measured by the QC laser-based sensor. The sensor was briefly connected to a cylinder that contained a 100-ppm NH$_3$:N$_2$ mixture, which resulted in a high ammonia peak. The thick curve on the expanded part of the plot depicts the Kalman-filtered results for NH$_3$ levels of <2 ppm.

continuously in bioreactor vent gases for more than 72 h at the NASA Johnson Space Center. The detected NH$_3$ concentration never exceeded a 0.5-ppm level, which was considered satisfactory in terms of bioreactor performance and agreed with concentrations measured by an indirect chemical method (see details in Ref. 8 and references therein).

4. Conclusions

We designed a compact portable ammonia sensor based on a thermoelectrically cooled pulsed QC DFB laser that operates at ~10 μm. This device was applied to real-world NH$_3$ concentration measurements. Furthermore, the configuration of this sensor will serve as the basis for the design of future portable QC DFB laser-based gas sensors for single or multiple trace gas quantification. The current sensitivity can be considerably improved by the addition of a second (reference) infrared detector. Such a two-beam configuration will cancel the noise caused by laser shot-to-shot energy fluctuations. These shot-to-shot fluctuations are the predominant noise source in our measurements. Furthermore, the use of such a reference channel would also eliminate baseline uncertainty. A number of additional improvements to the sensor are being planned. These include an increase in the pulse rate to 1 MHz, elimination of the need for a liquid-nitrogen-cooled detector, replacement of the general-purpose laboratory electronic devices with dedicated circuits, and use of advanced analog preprocessing of signals prior to digitization.

References

1. F. Capasso, C. Gmachl, R. Paiella, A. Tredicucci, A. L. Hutchinson, D. L. Sivco, J. N. Baillargeon, A. Y. Cho, and H. C. Liu, "New frontiers in quantum cascade lasers and applications," IEEE J. Sel. Top. Quantum Electron. **6,** 931–946 (2000).

2. C. Gmachl, F. Capasso, R. Köhler, A. Tredicucci, A. L. Hutchinson, D. L. Sivco, J. N. Baillargeon, and A. Y. Cho, "The senseability of semiconductor lasers," Circuits & Devices 10–18 (May 2000).

3. K. Namjou, S. Cai, E. A. Whittaker, J. Faist, C. Gmachl, F. Capasso, D. L. Sivco, and A. Y. Cho, "Sensitive absorption spectroscopy with a room-temperature distributed-feedback quantum-cascade laser," Opt. Lett. **23,** 219–221 (1997).

4. A. A. Kosterev, F. K. Tittel, C. Gmachl, F. Capasso, D. L. Sivco, J. N. Baillargeon, A. L. Hutchinson, and A. Y. Cho, "Trace-gas detection in ambient air with a thermoelectrically cooled, pulsed quantum-cascade distributed feedback laser," Appl. Opt. **39,** 6866–6872 (2000).

5. J. B. McManus, M. Zahniser, D. Nelson, and C. Kolb, "Recent laser spectroscopic systems developments at Aerodyne Research, Inc.," presented at the Third International Conference on Tunable Diode Laser Spectroscopy, 8–12 July 2001, Zermatt, Switzerland.

6. Anatoliy A. Kosterev, Alexander L. Malinovsky, Frank K. Tittel, Claire Gmachl, Federico Capasso, Deborah L. Sivco, James N. Baillargeon, Albert L. Hutchinson, and Alfred Y. Cho, "Cavity ringdown spectroscopic detection of nitric oxide with a continuous-wave quantum-cascade laser," Appl. Opt. **40,** 5522–5529 (2001).

7. R. Claps, D. Leleux, F. V. Englich, F. K. Tittel, M. E. Webber, J. B. Jeffries, R. K. Hanson, J. C. Graf, and L. M. Vega, "Infrared overtone spectroscopy of ammonia and carbon dioxide in the effluent of a biological water processor," in *Proceedings of 31st International Conference on Environmental Systems* (*IC-ES*) (Society of Automotive Engineers, 400 Commonwealth Dr., Warrendale, Pa. 15096-0001, 2001).

8. R. Claps, F. V. Englich, D. Leleux, D. Richter, F. K. Tittel, and R. F. Curl, "Ammonia detection by use of near-infrared diode-laser-based overtone spectroscopy," Appl. Opt. **40,** 4387–4394 (2001).

9. L. S. Rothman, C. P. Rinsland, A. Goldman, S. T. Massie, D. P. Edwards, J.-M. Flaud, A. Perrin, C. Camy-Peyret, V. Dana, J.-Y. Mandin, J. Schroeder, A. McCann, R. R. Gamache, R. B. Wattson, K. Yoshino, K. V. Chance, K. W. Jucks, L. R. Brown, V. Nemtchinov, and P. Varanasi, "The HITRAN molecular spectroscopic database and HAWKS (HITRAN Atmospheric Workstation): 1996 edition," J. Quant. Spectrosc. Radiat. Transfer **60,** 665–710 (1998).

10. M. E. Webber, D. S. Baer, and R. Hanson; "Ammonia monitoring near 1.5 μm with diode-laser absorption sensors," Appl. Opt. **40,** 2031–2042 (2001).

11. R. E. Kalman, "A new approach to linear filtering and prediction problems," J. Basic Eng. **82,** 35–42 (1960).

12. H. Riris, C. B. Carlisle, and R. E. Warren; "Kalman filtering of tunable diode laser spectrometer absorbance measurements," Appl. Opt. **33,** 5506–5508 (1994).

13. D. P. Leleux, R. Claps, W. Chen, F. K. Tittel, and T. L. Harman, "Adaptive filtering applications to realtime simultaneous CO_2 and NH_3 measurements," Appl. Phys. B (to be published). (2001).